European Journal of Medicinal Chemistry 46 (2011) 1066–1073

Contents lists available at ScienceDirect

European Journal of Medicinal Chemistry

journal homepage: http://www.elsevier.com/locate/ejmech

Original article

Synthesis and structure–activity relationship of N-(2-arylethyl) isoquinoline derivatives as human scavenger receptor CD36 antagonists

Yan-Xiang Wang [1], Li Wang [1], Yan-Ni Xu, Ying-Hong Li, Jian-Dong Jiang, Shu-Yi Si, Yang-Biao Li, Gang Ren, Yong-Qiang Shan, Bin Hong**, Dan-Qing Song*

Institute of Medicinal Biotechnology, Chinese Academy of Medical Sciences and Peking Union Medical College, Beijing 100050, China

ARTICLE INFO

Article history:
Received 16 September 2010
Received in revised form
5 January 2011
Accepted 12 January 2011
Available online 21 January 2011

Keywords:
N-(2-Arylethyl) isoquinoline
CD36 Antagonist
Oxidized low density lipoprotein
Structure–activity relationship

ABSTRACT

By using human scavenger receptor CD36 as the target, twenty-five N-(2-arylethyl) isoquinoline derivatives were designed, synthesized and evaluated for their antagonistic activities for CD36-oxidatively low density lipoprotein (oxLDL) binding. The primary analysis of structure–activity relationship (SAR) indicated a methoxyl at the 7-position and a hydroxyl at the 6- or 8-position could afford good activities. Among these analogs, compounds **7e** and **7t** showed the potential CD36 antagonistic activities with IC_{50} values of 0.2 and 0.8 μg/mL, respectively. Furthermore, both of them could effectively inhibit oxLDL uptake in insect Sf9 cells overexpressing human CD36, and thus have been selected for further investigation. We consider N-(2-arylethyl) isoquinoline analogs to be a family of novel CD36 antagonists.

1. Introduction

Atherosclerosis (AS) is a progressive chronic inflammatory disease characterized by a gradual thickening and hardening of the arterial wall and becomes the primary cause of coronary artery and cerebrovascular disease. Binding and uptake of oxidatively low density lipoproteins (oxLDL) by macrophages is one of the earliest steps in the development of atherosclerotic lesions and lipid-laden foam cells that constitute the atherosclerotic lesion core [1–3]. Monocyte/macrophage CD36, as a scavenger receptor, has been shown to play a critical role in the development of atherosclerotic lesions by its capacity to bind and endocytose oxLDL into macrophages, which is implicated in the formation of foam cells [4–8].

CD36 is a member of the multi-ligand scavenger receptor class B family present on the surface of a number of cells such as platelets, monocytes/macrophages, endothelial and smooth muscle cell [9,10]. Since CD36 was discovered as a macrophage receptor for oxLDL, it could played a major role in the initiation of atherosclerotic process and be considered as the target against AS [11,12]. Therefore, CD36 antagonists might be useful in blocking oxLDL-CD36 binding and be developed to a novel class of anti-atherosclerotic agents. The screening of small molecule CD36 antagonists may be one of the approaches to discover the potential drug candidates against AS [13].

During the course of synthesis of berberine (BBR, Fig. 1) analogs as a kind of LDLR mRNA up-regulators [14–16], a new class of compound, 7-hydroxy-2-{2-[3-(trifluoromethyl)phenyl]ethyl}isoquinolinium chloride (**1**, Fig. 1) was obtained accidently and identified structurally. However, compound **1** lost its activity on up-regulatory LDLR expression in comparison with BBR (data not shown). The factor contributes to the activity loss is presumable the configurational change of BBR and **1**. The planar structure converted into bended one at the carbon–carbon single bond between the ring A and C. Screened by the models developed in our laboratory, we found that compound **1** showed a potential antagonistic activity for CD36-oxLDL binding with IC_{50} value of 1.2 μg/mL much greater than that of positive control hexarelin (Fig. 1) with IC_{50} value of 46.8 μg/mL [17].

The novel biological activity and unique chemical structure of **1** provoked our strong interest to explore the structure–activity relationship (SAR) of this kind of compounds for CD36-oxLDL antagonistic activities. Taking compound **1** as the lead, we initiated the SAR analysis on the modifications of substituents on the ring D, A and C, respectively, on which twenty-five new isoquinoline derivatives were designed, synthesized and evaluated for their antagonistic activities for CD36-oxLDL binding in the present study.

* Corresponding author. Tel./fax: +86 10 6316 5268.
** Corresponding author. Tel./fax: +86 10 6302 8003.
E-mail addresses: binhong69@hotmail.com (B. Hong), songdanqingsdq@hotmail.com (D.-Q. Song).
[1] These authors made equal contributions to the work.

0223-5234/$ – see front matter © 2011 Elsevier Masson SAS. All rights reserved.
doi:10.1016/j.ejmech.2011.01.022

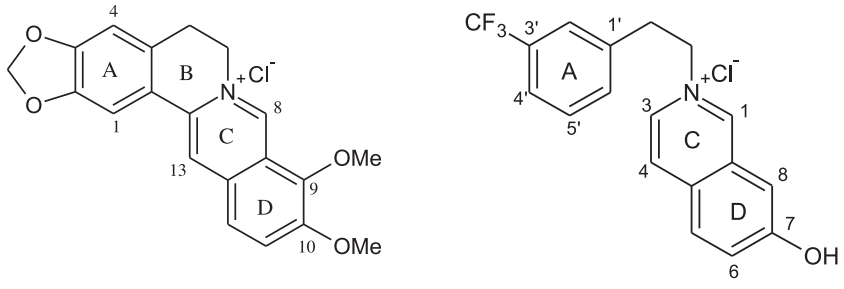

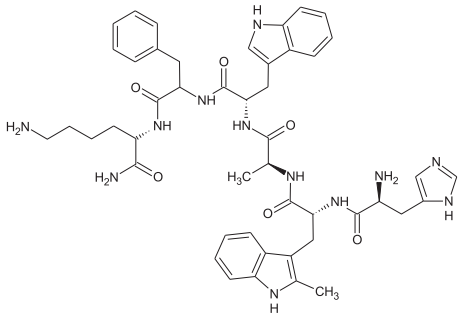

Fig. 1. Chemical structures of BBR, **1** and hexarelin.

2. Chemistry

The twenty-five compounds were synthesized through a four-step process (Scheme 1), using commercially available derivatives of phenylethylamine (**2**) and benzaldehyde (**3**) as starting materials with the methods reported previously [14–16]. In the intermolecular cyclization of the intermediate **5**, ring B could not cyclize without assistance of activating groups (such as hydroxyl, methyl or methoxyl) at the 3′- or 5′-position of the ring A according to Pictet–Spengler reaction rule, and subsequently the key intermediate **6** would be obtained with the yields of 28–53%. The crude products in **7** series were prepared by the acidification of intermediate **6**. The final products (**7a**–**v**) were purified via flash column chromatography using methanol/dichloromethane as the eluent. In the other hand, the ring B and C might form simultaneously while an activating group exists at the same position on the ring A, thus BBR analogs were synthesized [14–16].

In the course of intermolecular cyclization of **5**, another key intermediate **8** was obtained as well, when the amount of the dehydrating agent-$CuSO_4$ was deduced to half level and the cyclization time was shortened from 5 h to 1 h. The final products (**9a**–**c**) were obtained with the same procedures of **7** series with a good yield.

3. Results and discussion

3.1. SAR analysis for the CD36 antagonistic activity

The high throughput screening (HTS) of enzyme-linked immunosorbent assay (ELISA)-like constructed in our laboratory [17] was used for initial biological screening at the level of CD36-ligand binding. The extracellular domain of human CD36 expressed in *Escherichia coli* as a His-tagged protein, had been demonstrated to bind oxLDL specifically. Structures of the twenty-five analogs and their antagonistic activities for CD36-oxLDL binding with hexarelin as a positive control are shown in Table 1.

The SAR study was first focused on the substituents on the aromatic ring A and D of compound **1**. Retaining the hydroxyl at the 7-position and replacing trifluoromethyl with a hydrogen, fluoro or methoxyl at position 2′ or 4′, respectively, by which three analogs (**7a**–**c**) were created. The results showed that all of them lost their antagonistic activities on CD36 partially or completely. Instead of the hydroxyl of **7a** with a methoxyl at position 7 (**7d**) afforded a moderated activity similar to that of **1**. It seems that the methoxyl at position 7 might be beneficial for the activity.

Next, SAR analysis was concentrated on the di-substituted side-chains of the ring D. Retainment of the methoxyl at position 7 and introduction of a hydroxyl at the 8-position, with which four analogs (**7e**–**h**) were synthesized. Compound **7e** without substituents on the ring A afforded the most potent activity in CD36 antagonism with about 1.6-fold increase over that of **1**. Other compounds (**7f**–**h**) bearing a methyl, fluoro or methoxyl at the 2′- or 4′-position exhibited a partial or complete loss in CD36 antagonistic activities.

In another variation, dimethoxy was attached at the 7-, 8-positions of the ring D, from which four compounds (**7i**–**l**) were generated. Compounds **7j**–**k** possessing a methyl or fluoro at the 2′- or 3′-position respectively had activities similar to that of **1**. Compound **7i** and **7l** showed decreased antagonistic activities on CD36. Additionally, moving the methoxyl from the 8- to 6-position, five analogs (**7m**–**q**) were obtained. The results showed that movement of the methoxyl from the 8- to 6-position on the ring D resulted in a partial or complete loss of activity regardless of the size, position and electronic effect of groups on the ring A.

Furthermore, replacing the methoxyl with a hydroxyl at the 6-position, compounds **7r**–**v** bearing a hydrogen, fluoro, chloro or methoxyl at the 3′- or 4′-position, respectively, were made and tested. Compound **7t** with 4′-methoxyl showed a CD36

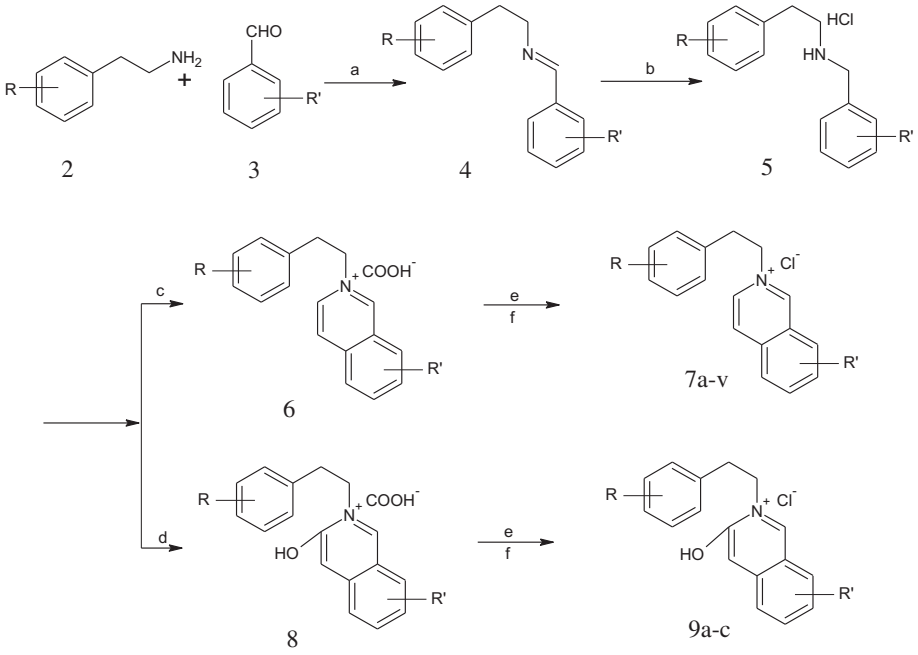

Scheme 1. Synthesis of the study compounds. Reagents and conditions: (a) 70 °C, 1 h; (b) $NaBH_4$, methanol, reflux, 4 h; (c) glyoxal, formic acid, $CuSO_4$, HCl, 100 °C, 5 h; (d) glyoxal, formic acid, $CuSO_4$, HCl, 100 °C, 1 h; (e) methanol/H_2O, CaO, r.t., 2 h; (f) ethanol/HCl, r.t., 0.5 h.

antagonistic activity greater than **1** did. Also, compound **7u** possessing a fluoro at the same position exhibited a moderated activity in respect to **1**. We therefore deduced that a methoxyl and hydroxyl at the 7- and 6-position, respectively, was an optimal combination for the structure in their antagonistic activity on CD36.

The preliminary SAR analysis of ring B was carried out as well. We retained the active fragment of the ring D, i.e. 7-methoxyl and 8-hydroxyl, and introduced a hydroxyl at the 3-position of the ring C, with which three compounds (**9a**–**c**) were designed and synthesized. The results showed that all of them almost lost their activities on CD36. We considered the quaternary ammonium ion at the 2-position to be an important role in binding to speculated biological targets. The lone pair electrons in hydroxyl at position 3 might form an electrostatic attraction with quaternary ammonium ion and reduce its electro-positivity, and subsequently interfere with the bioactivity of the analogs.

Among those analogs, the compounds **7e**, **7j**–**k** and **7t**–**u** afforded the potential CD36 antagonistic effects in comparison with **1**, and thus their dose-dependent competition assays were further performed. As shown in Fig. 2, the five compounds showed CD36 antagonistic effect with IC_{50} values ranging from 0.2 to 2.4 μg/mL. Especially, compounds **7e** and **7t** are the promising CD36 antagonists with IC_{50} values of 0.2 and 0.8 μg/mL, respectively.

3.2. The CD36 antagonistic effect at the cellular level

To confirm the effects of the compounds (**1**, **7e**, **7j**–**k**, **7t**–**u**) screened from the above HTS assay, the assay for CD36 antagonists in *Spodoptera frugiperda* (Sf9) cells overexpressing human CD36 (Sf9[hCD36]) developed in our laboratory [18] was used to examine the activities of the hits. OxLDL (40 μg/mL) was used as a positive control, and its inhibitory activity was defined as 100%. As shown in Fig. 3, all of them could inhibit 1, 10-dioctadecyl-3, 3, 30, 30-tetramethylindocarbo cyanine perchlorate labeled acetylated LDL (DiI-AcLDL) uptake in Sf9[hCD36] cells at different levels, and their activities were just agreeable with those in CD36-oxLDL binding assay. The results indicated that the compounds could inhibit natural ligands binding CD36 at both cellular and molecular levels.

3.3. Fluorescence microscopic analysis

Since compounds **7e** and **7t** afforded the potential CD36 antagonistic activities, and thus their antagonistic effect was further examined using fluorescence microscopy in Sf9[hCD36] cells. The amounts of fluorescence in the cells incubated with DiI-AcLDL (5 μg/mL) plus compounds **7t** or **7e** (10 μg/mL) were obviously lower (Fig. 4C,D) than those in the cells with DiI-AcLDL alone (Fig. 4A), suggesting that both of them could inhibit DiI-AcLDL uptake in Sf9[hCD36] cells by antagonizing CD36-oxLDL binding. OxLDL (40 μg/mL) was used as positive control, and there was no fluorescence uptake (Fig. 4B).

4. Conclusion

In conclusion, we have synthesized twenty-five N-(2-arylethyl) isoquinoline analogs with different substituents on the ring A, B or C and studied the biological effect as CD36 antagonists. The results suggested that the compounds with a methoxyl at position 7 and a hydroxyl at the 6- or 8-position showed the potent activities. The hydroxyl at either 6- or 8-position might provide a beneficial shoring effect for the 7-methoxyl to obtain an optimal steric conformation. These results are of interest to establish the SAR of N-(2-arylethyl) isoquinoline analogs, and provide the basis for further chemical investigation. As compounds **7e** and **7t** showed the potential antagonistic activities for CD36-oxLDL binding on both the molecular and cellular levels, they have been selected for the next-step evaluation in animal experiments.

5. Experimental section

5.1. Chemistry

Unless otherwise noted, all commercial reagents and solvents were obtained from the commercial provider and used without further purification. ^1H NMR and ^{13}C NMR spectra were recorded on Varian 400 MHz spectrometers. Chemical shifts were reported relative to internal tetramethylsilane. Flash column chromatography was

Table 1
CD36 receptor antagonistic effect of study analogs.

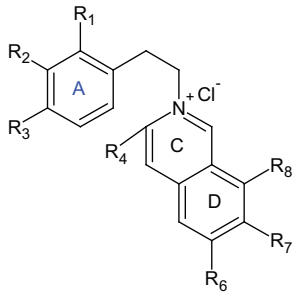

Compd	R_1	R_2	R_3	R_4	R_6	R_7	R_8	Inhibition rate (%)[a]
Hexarelin[b]								37.6 ± 1.8
1	H	CF_3	H	H	H	OH	H	48.4 ± 3.7
7a	H	H	H	H	H	OH	H	<10
7b	F	H	H	H	H	OH	H	21.7 ± 3.8
7c	H	H	OCH_3	H	H	OH	H	28.7 ± 4.0
7d	H	H	H	H	H	OCH_3	H	47.4 ± 2.6
7e	H	H	H	H	H	OCH_3	OH	77.9 ± 11.5
7f	CH_3	H	H	H	H	OCH_3	OH	11.5 ± 6.2
7g	H	H	F	H	H	OCH_3	OH	29.6 ± 15.7
7h	H	H	OCH_3	H	H	OCH_3	OH	<10
7i	H	H	H	H	H	OCH_3	OCH_3	<10
7j	CH_3	H	H	H	H	OCH_3	OCH_3	46.6 ± 4.8
7k	H	F	H	H	H	OCH_3	OCH_3	52.1 ± 13.4
7l	H	H	Cl	H	H	OCH_3	OCH_3	25.4 ± 5.6
7m	H	H	H	H	OCH_3	OCH_3	H	10.0 ± 1.0
7n	H	F	H	H	OCH_3	OCH_3	H	20.9 ± 3.3
7o	H	CF_3	H	H	OCH_3	OCH_3	H	<10
7p	H	H	OCH_3	H	OCH_3	OCH_3	H	28.6 ± 1.2
7q	H	H	Cl	H	OCH_3	OCH_3	H	<10
7r	H	H	H	H	OH	OCH_3	H	31.0 ± 3.0
7s	H	Cl	H	H	OH	OCH_3	H	33.6 ± 9.8
7t	H	H	OCH_3	H	OH	OCH_3	H	76.3 ± 2.0
7u	H	H	F	H	OH	OCH_3	H	42.4 ± 17.6
7v	H	H	Cl	H	OH	OCH_3	H	<10
9a	H	Cl	H	OH	OH	OCH_3	H	33.2 ± 7.3
9b	CH_3	H	H	OH	OH	OCH_3	H	<10
9c	H	F	H	OH	OH	OCH_3	H	<10

[a] OxLDL (5 μg/mL) was first coated and then blocked with 1% BSA. Later, CD36 (30 μg/mL) was added to incubate with hexarelin (10 μM) and study compounds (10 μg/mL) for 2 h. The inhibition of oxLDL binding with CD36 was determined by OD_{450} values. The untreated control was defined as **1**, and the inhibition of analogs was calculated with the formulation: inhibition rate (%) = (1 − OD_{450} of compounds/OD_{450} of untreated control) × 100. The data shown were mean values of at least 3 separate experiments.

[b] The concentration of hexarelin was 10 μM.

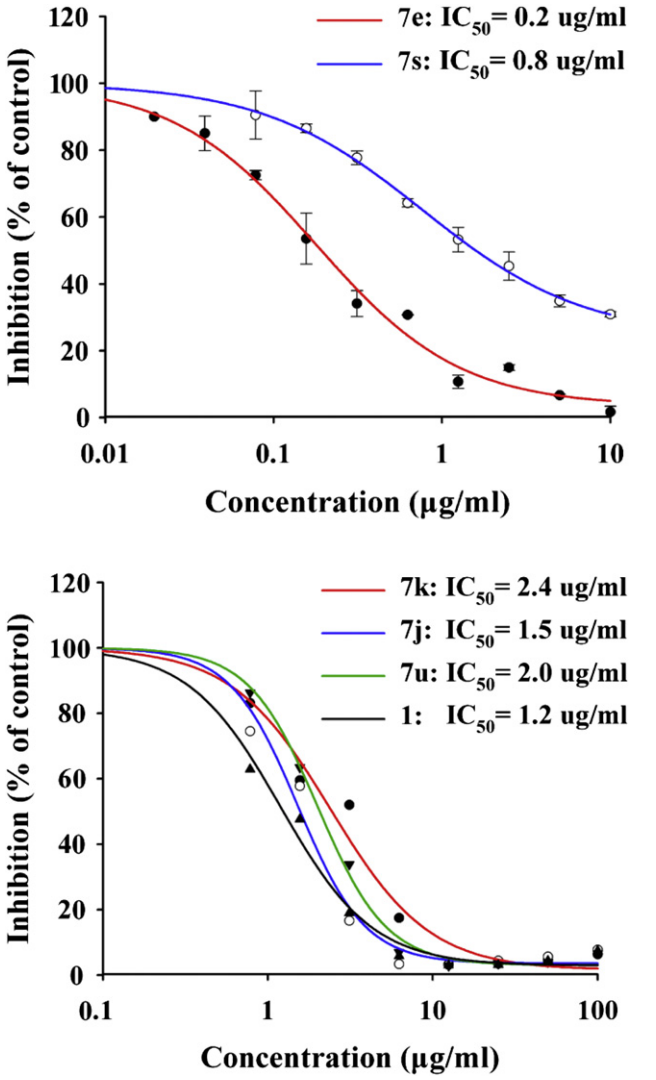

Fig. 2. The dose-response curves of the active compounds (10 μg/mL) for CD36-oxLDL antagonistic effect.

performed on 200–400 mesh silica gel. Thin layer chromatography (TLC) was performed using E. Merck silica gel 60 F254 precoated plates. Melting points (m.p.) are uncorrected and were recorded on a Büchi capillary melting point apparatus.

*5.1.1. General procedure for N-(2-arylethyl) isoquinolines analogs (**7a–v**)*

A 250 mL round bottom flask was charged with **2** (1.0 equiv) and **3** (1.0 equiv) at 70 °C, and the mixture was stirred under vacuum for 1 h. Methanol (100 mL) was added to the residue, and then $NaBH_4$ (3.0 equiv) was added portionwise at the r.t. The mixture was refluxed for 4 h. Upon completion, as determined by TLC, the reaction mixture was concentrated *in vacuo*. The residue was dissolved in water (300 mL). The resulting aqueous phase was extracted with ethyl acetate (3 × 100 mL) and the combined organic layers were rinsed with saturated brines (100 mL) and dried (Na_2SO_4). Concentrated hydrochloric acid was added dropwise to adjust PH of the organic layer to 5–6, and filtered to give the hydrochlorate (**5**) without further purification.

To a suspension of anhydrous $CuSO_4$ (3.6 equiv) and **5** (1.0 equiv) in anhydrous formic acid (45 mL) was added glyoxal (40%, 2.0 equiv) at 100 °C. The reaction mixture was stirred at 100 °C for 5 h, concentrated hydrochloric acid (0.8 and 0.6 equiv) was added at 2 h and 4 h respectively during this process. Upon completion, as determined by TLC, the mixture was filtered. The filtrate was concentrated *in vacuo*. The residue (**6**) was dissolved in methanol (500 mL) and water (10 mL), CaO was added portionwise to adjust PH to 9–10. The suspension was stirred at the r.t. for 2 h, filtered and concentrated *in vacuo*. The resulting residues were purified via flash column chromatography using methanol/dichloromethane as the eluent, and then acidified by 10% HCl/ethanol to give **7**.

*5.1.1.1. 7-Hydroxy-2-{2-[3-(trifluoromethyl)phenyl]ethyl}isoquinolinium chloride (**1**).* Yield: 42%; mp: 100–102 °C (decomp); Dark red solid; ^{1}H NMR (DMSO-d_6, ppm): δ 11.21 (s, br, 1H, OH), 9.73 (s, 1H, 8-CH), 8.54 (d, 1H, J = 6.8 Hz, Ph), 8.44 (d, 1H, J = 6.8 Hz, Ph), 8.20 (d, 1H, J = 8.8 Hz, Ph), 7.77 (d, 1H, J = 8.8 Hz, Ph), 7.54 (m, 5H, Ph), 4.91 (t, 2H, J = 7.6 Hz, CH_2), 3.44 (t, 2H, J = 7.6 Hz, CH_2). HRMS-ESI calcd for $C_{18}H_{15}NOF_3Cl$: 319.1184 $[M + H - Cl]^+$, found 319.1171.

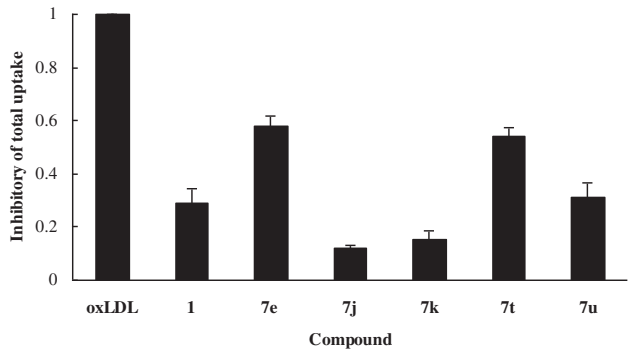

Fig. 3. CD36 antagonistic activities of the active compounds in Sf9[hCD36] cells. OxLDL was used as a positive control. The cellular uptake of DiI-AcLDL was determined in the treatment of compounds (10 μg/mL). Presented are means and sds.

*5.1.1.2. 7-Hydroxy-2-(2-phenylethyl)isoquinolinium chloride (**7a**).* Yield: 51%; mp: 124–126 °C (decomp); Orange solid; ^{1}H NMR (DMSO-d_6, ppm): δ 11.50 (s, br, 1H, OH), 9.94 (s, 1H, 8-CH), 8.56 (d, 1H, J = 6.8 Hz, Ph), 8.40 (d, 1H, J = 6.8 Hz, Ph), 8.18 (d, 1H, J = 8.8 Hz, Ph), 7.80 (d, 1H, J = 8.8 Hz, Ph), 7.63 (s, 1H, Ph), 7.28–7.19 (m, 5H, Ph), 4.91 (t, 2H, J = 7.2 Hz, CH_2), 3.40 (t, 2H, J = 7.2 Hz, CH_2). ^{13}C NMR (DMSO-d_6, ppm): δ 172.7, 164.1, 162.2, 157.4, 138.6, 136.6, 132.2, 130.0, 128.7 (2), 128.6 (2), 126.9, 121.3, 114.5, 61.3, 33.2. HRMS-ESI calcd for $C_{17}H_{16}NOCl$: 250.1232 $[M - Cl]^+$, found 250.1231.

*5.1.1.3. 7-Hydroxy-2-[2-(4-methoxyphenyl)ethyl]isoquinolinium chloride (**7b**).* Yield: 43%; mp: 118–120 °C (decomp); Orange solid; ^{1}H NMR (DMSO-d_6, ppm): δ 9.10 (s, 1H, 8-CH), 7.96 (s, 2H, Ph), 7.50 (d, 1H, J = 8.8 Hz, Ph), 7.32 (d, 1H, J = 8.8 Hz, Ph), 7.14 (s, 1H, Ph), 7.12 (s, 1H, Ph), 6.83 (s, 1H, Ph), 6.81 (s, 1H, Ph), 6.70 (s, 1H, OH), 4.67 (t, 2H, J = 6.8 Hz, CH_2), 3.68 (s, 3H, OCH_3), 3.20 (t, 2H, J = 6.8 Hz, CH_2). HRMS-ESI calcd for $C_{18}H_{18}NO_2Cl$: 280.1338 $[M - Cl]^+$, found 280.1343.

*5.1.1.4. 2-[2-(2-Fluorophenyl)ethyl]-7-hydroxyisoquinolinium chloride (**7c**).* Yield: 36%; mp: 97–99 °C (decomp); Brown solid; ^{1}H NMR (DMSO-d_6, ppm): δ 11.22 (s, br, 1H, OH), 9.70 (s, 1H, 8-CH), 8.51 (d, 1H, J = 6.8 Hz, Ph), 8.41 (d, 1H, J = 6.8 Hz, Ph), 8.20 (d, 1H, J = 7.2 Hz, Ph), 7.77 (d, 1H, J = 7.2 Hz, Ph), 7.52 (s, 1H, Ph), 7.22 (m, 2H, Ph), 7.05 (m, 2H, Ph), 4.89 (t, 2H, J = 7.2 Hz, CH_2), 3.31 (t, 2H, J = 7.2 Hz, CH_2). HRMS-ESI calcd for $C_{17}H_{15}NOFCl$: 268.1138 $[M - Cl]^+$, found 268.1140.

*5.1.1.5. 7-Methoxy-2-(2-phenylethyl)isoquinolinium chloride (**7d**).* Yield: 43%; Brown oil; ^{1}H NMR (DMSO-d_6, ppm): δ 9.80 (s, 1H, 8-CH), 8.65 (d, 1H, J = 6.4 Hz, Ph), 8.49 (d, 1H, J = 6.4 Hz, Ph), 8.26 (d, 1H, J = 9.2 Hz, Ph), 7.88 (d, 1H, J = 9.2 Hz, Ph), 7.72 (s, 1H, Ph), 7.28–7.21(m, 5H, Ph), 4.96 (t, 2H, J = 7.6 Hz, CH_2), 3.98 (s, 3H, OCH_3), 3.53 (t, 2H, J = 7.6 Hz, CH_2). HRMS-ESI calcd for $C_{18}H_{18}NOCl$: 264.1388 $[M - Cl]^+$, found 264.1379.

*5.1.1.6. 8-Hydroxy-7-methoxy-2-(2-phenylethyl)isoquinolinium chloride (**7e**).* Yield: 28%; mp: 78–80 °C; Brown solid; ^{1}H NMR (DMSO-d_6, ppm): δ 9.95 (s, 1H, 8-CH), 8.35 (d, 1H, J = 6.8 Hz, Ph), 8.07 (d, 1H, J = 6.8 Hz, Ph), 7.83 (s, 1H, Ph), 7.78 (s, 1H, Ph), 7.31–7.24 (m, 5H, Ph), 6.98 (s, 1H, OH), 4.81 (t, 2H, J = 6.4 Hz, CH_2), 3.88 (s, 3H, OCH_3), 3.03 (t, 2H, J = 6.4 Hz, CH_2). HRMS-ESI calcd for $C_{18}H_{18}NO_2Cl$: 280.1338 $[M - Cl]^+$, found 280.1357.

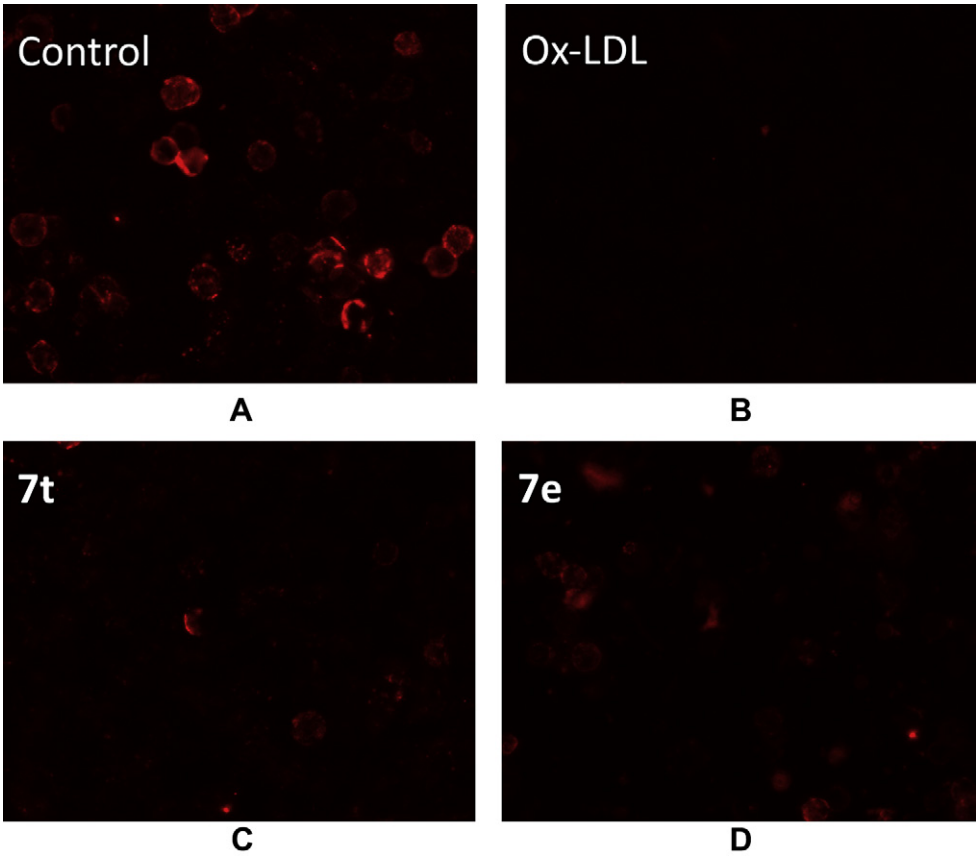

Fig. 4. The Sf9[hCD36] cells were incubated with DiI-AcLDL (5 μg/mL) and compounds **7t**, **7e** for 6 h, and then examined by confocal fluorescence microscopy (10×magnification).

*5.1.1.7. 8-Hydroxy-7-methoxy-2-[2-(4-methoxyphenyl)ethyl]isoquinolinium chloride (**7f**).* Yield: 46%; mp: 145–147 °C (decomp); Red solid; ^{1}H NMR (DMSO-d$_6$, ppm): δ 9.05 (s, 1H, 8-CH), 7.65 (d, 1H, *J* = 6.8 Hz, Ph), 7.51 (d, 1H, *J* = 6.8 Hz, Ph), 7.26 (s, 1H, Ph), 7.18 (s, 1H, Ph), 7.16 (s, 1H, Ph), 7.14 (s, 1H, Ph), 6.84 (s, 1H, Ph), 6.82 (s, 1H, Ph), 6.41 (s, 1H, OH), 4.49 (t, 2H, *J* = 7.2 Hz, CH$_2$), 3.73 (s, 3H, OCH$_3$), 3.69 (s, 3H, OCH$_3$), 3.08 (t, 2H, *J* = 7.2 Hz, CH$_2$). HRMS-ESI calcd for $C_{19}H_{20}NO_3Cl$: 310.1443 [M − Cl]$^+$, found 310.1444.

*5.1.1.8. 2-[2-(4-Fluorophenyl)ethyl]-8-hydroxy-7-methoxyisoquinolinium chloride (**7g**).* Yield: 32%; mp: 77–79 °C (decomp); Dark red solid; ^{1}H NMR (DMSO-d$_6$, ppm): δ 9.54 (s, 1H, 8-CH), 8.24 (d, 1H, *J* = 6.8 Hz, Ph), 8.01 (d, 1H, *J* = 6.8 Hz, Ph), 7.84 (s, 1H, Ph), 7.29 (m, 3H, Ph), 7.13 (m, 3H, Ph), 4.77 (t, 2H, *J* = 7.2 Hz, CH$_2$), 3.91 (s, 3H, OCH$_3$), 3.22 (t, 2H, *J* = 7.2 Hz, CH$_2$). ^{13}C NMR (DMSO-d$_6$, ppm):δ 162.4, 160.0, 147.5, 145.9, 132.7, 132.0, 131.0, 126.5, 123.3, 120.2, 119.6, 115.4 (2), 115.2 (2), 56.9, 55.6, 35.6. HRMS-ESI calcd for $C_{18}H_{17}NO_2FCl$: 298.1243 [M − Cl]$^+$, found 298.1244.

*5.1.1.9. 8-Hydroxy-7-methoxy-2-[2-(2-methylphenyl)ethyl]isoquinolinium chloride (**7h**).* Yield: 37%; mp: 261–263 °C (decomp); Dark red solid; ^{1}H NMR (DMSO-d$_6$, ppm): δ 8.98 (s, 1H, 8-CH), 7.58 (d, 1H, *J* = 6.8 Hz, Ph), 7.45 (d, 1H, *J* = 6.8 Hz, Ph), 7.20 (d, 1H, *J* = 7.6 Hz, Ph), 7.11–7.14 (m, 5H, Ph), 6.32 (d, 1H, *J* = 6.8 Hz, Ph), 4.47 (t, 2H, *J* = 7.6 Hz, CH$_2$), 3.71 (s, 3H, OCH$_3$), 3.31 (t, 2H, *J* = 7.6 Hz, CH$_2$), 2.28 (s, 3H, CH$_3$). HRMS-ESI calcd for $C_{19}H_{20}NO_2Cl$: 294.1494 [M − Cl]$^+$, found 294.1499.

*5.1.1.10. 7,8-Dimethoxy-2-(2-phenylethyl)isoquinolinium chloride (**7i**).* Yield: 58%; mp: 90–92 °C; Yellow solid; ^{1}H NMR (DMSO-d$_6$, ppm): δ 9.68 (s, 1H, 8-CH), 8.66 (d, 1H, *J* = 7.0 Hz, Ph), 8.10 (d, 1H, *J* = 7.0 Hz, Ph), 8.22 (d, 1H, *J* = 9.0 Hz, Ph), 8.09 (d, 1H, *J* = 9.0 Hz, Ph), 7.28–7.21 (m, 5H, Ph), 5.02 (t, 2H, *J* = 7.5 Hz, CH$_2$), 4.05 (s, 3H, OCH$_3$), 3.97 (s, 3H, OCH$_3$), 3.43 (t, 2H, *J* = 7.5 Hz, CH$_2$). HRMS-ESI calcd for $C_{19}H_{20}NO_2Cl$: 294.1494 [M − Cl]$^+$, found 294.1494.

*5.1.1.11. 7,8-Dimethoxy-2-[2-(2-methylphenyl)ethyl]isoquinolinium chloride (**7j**).* Yield: 39%; Brown oil; ^{1}H NMR (DMSO-d$_6$, ppm): δ 9.60 (s, 1H, 8-CH), 8.61 (d, 1H, *J* = 6.4 Hz, Ph), 8.49 (d, 1H, *J* = 6.8 Hz, Ph), 8.23 (d, 1H, *J* = 9.2 Hz, Ph), 8.10 (d, 1H, *J* = 8.8 Hz, Ph), 7.14 (m, 2H, Ph), 7.01 (m, 2H, Ph), 4.97 (t, 2H, *J* = 7.2 Hz, CH$_2$), 4.05 (s, 3H, OCH$_3$), 3.94 (s, 3H, OCH$_3$), 3.09 (t, 2H, *J* = 7.2 Hz, CH$_2$), 2.24 (s, 3H, CH$_3$). HRMS-ESI calcd for $C_{20}H_{22}NO_2Cl$: 309.1729 [M + H − Cl]$^+$, found 309.1720.

*5.1.1.12. 2-[2-(3-Fluorophenyl)ethyl]-7,8-dimethoxyisoquinolinium chloride (**7k**).* Yield: 46%; Dark brown oil; ^{1}H NMR (DMSO-d$_6$, ppm): δ 9.75 (s, 1H, 8-CH), 8.61 (d, 1H, *J* = 6.4 Hz, Ph), 8.50 (d, 1H, *J* = 6.4 Hz, Ph), 8.23 (d, 1H, *J* = 8.8 Hz, Ph), 8.09 (d, 1H, *J* = 8.8 Hz, Ph), 7.30 (dd, 1H, *J* = 8.0 Hz, *J* = 14.4 Hz, Ph), 7.18 (d, 1H, *J* = 10.0 Hz, Ph), 7.05 (m, 2H, Ph), 5.01 (t, 2H, *J* = 7.2 Hz, CH$_2$), 4.05 (s, 3H, OCH$_3$), 3.99 (s, 3H, OCH$_3$), 3.35 (t, 2H, *J* = 7.2 Hz, CH$_2$). HRMS-ESI calcd for $C_{19}H_{19}NO_2FCl$: 313.1478 [M + H − Cl]$^+$, found 313.1465.

*5.1.1.13. 2-[2-(4-Chlorophenyl)ethyl]-7,8-dimethoxyisoquinolinium chloride (**7l**).* Yield: 43%; Yellow oil; ^{1}H NMR (DMSO-d$_6$, ppm): δ 9.73 (s, 1H, 8-CH), 8.63 (d, 1H, *J* = 6.4 Hz, Ph), 8.50 (d, 1H, *J* = 6.4 Hz, Ph), 8.23 (d, 1H, *J* = 8.8 Hz, Ph), 8.10 (d, 1H, *J* = 8.8 Hz, Ph), 7.35 (d, 2H, *J* = 8.0 Hz, Ph), 7.27 (d, 2H, *J* = 8.8 Hz, Ph), 5.00 (t, 2H, *J* = 7.2 Hz, CH$_2$), 4.01 (s, 3H, OCH$_3$), 3.99 (s, 3H, OCH$_3$), 3.36 (t, 2H, *J* = 7.2 Hz, CH$_2$). HRMS-ESI calcd for $C_{19}H_{19}NO_2Cl_2$: 328.1104 [M − Cl]$^+$, found 328.1103.

*5.1.1.14. 6,7-Dimethoxy-2-(2-phenylethyl)isoquinolinium chloride (**7m**).* Yield: 53%; mp: 124–126 °C; Light yellow solid; ^{1}H NMR (DMSO-d$_6$, ppm): δ 9.67 (s, 1H, 8-CH), 8.58 (d, 1H, *J* = 6.8 Hz, Ph), 8.26 (d, 1H, *J* = 6.8 Hz, Ph), 7.75 (s, 1H, Ph), 7.70 (s, 1H, Ph), 7.28–7.19 (m, 5H, Ph), 4.90 (t, 2H, *J* = 6.4 Hz, CH$_2$), 4.04 (s, 3H, OCH$_3$), 3.97 (s, 3H, OCH$_3$), 3.32 (t, 2H, *J* = 6.4 Hz, CH$_2$). HRMS-ESI calcd for $C_{19}H_{20}NO_2Cl$: 294.1494 [M − Cl]$^+$, found 294.1485.

*5.1.1.15. 2-[2-(3-Fluorophenyl)ethyl]-6,7-dimethoxyisoquinolinium chloride (**7n**).* Yield: 44%; mp: 106–108 °C (decomp); Orange solid; ^{1}H NMR (DMSO-d$_6$, ppm): δ 9.56 (s, 1H, 8-CH), 8.52 (d, 1H, *J* = 6.8 Hz, Ph), 8.26 (d, 1H, *J* = 6.8 Hz, Ph), 7.73 (s, 1H, Ph), 7.69 (s, 1H, Ph), 7.29 (dd, 1H, *J* = 7.6 Hz, *J* = 14.4 Hz, Ph), 7.15 (d, 1H, *J* = 10.0 Hz, Ph), 7.06 (t, 1H, *J* = 8.8 Hz, Ph), 7.00 (d, 1H, *J* = 6.4 Hz, Ph), 4.89 (t, 2H, *J* = 7.2 Hz, CH$_2$), 4.05 (s, 3H, OCH$_3$), 3.99 (s, 3H, OCH$_3$), 3.34 (t, 2H, *J* = 7.2 Hz, CH$_2$). ^{13}C NMR (DMSO-d$_6$, ppm): δ 160.9, 157.5, 152.4, 145.0, 139.3, 135.1, 133.5, 130.5, 125.1, 123.6, 123.1, 115.8, 113.8, 107.0, 105.8, 60.4, 56.8, 56.6, 36.0. HRMS-ESI calcd for $C_{19}H_{19}NO_2FCl$: 312.1340 [M − Cl]$^+$, found 312.1414.

*5.1.1.16. 6,7-Dimethoxy-2-{2-[3-(trifluoromethyl)phenyl]ethyl}isoquinolinium chloride (**7o**).* Yield: 51%; mp: 196–198 °C (decomp); Pale white solid; ^{1}H NMR (DMSO-d$_6$, ppm): δ 9.65 (s, 1H, 8-CH), 8.60 (d, 1H, *J* = 6.8 Hz, Ph), 8.29 (d, 1H, *J* = 6.8 Hz, Ph), 7.76 (s, 1H, Ph), 7.69 (s, 1H, Ph), 7.59–7.63 (m, 4H, Ph), 4.92 (t, 2H, *J* = 7.2 Hz, CH$_2$), 4.06 (s, 3H, OCH$_3$), 3.99 (s, 3H, OCH$_3$), 3.43 (t, 2H, *J* = 7.2 Hz, CH$_2$). ^{13}C NMR (DMSO-d$_6$, ppm): δ 157.6, 152.5, 145.2, 138.0, 137.2, 135.2, 133.6, 133.2, 129.6, 129.1, 125.6, 123.7, 123.2, 118.0, 106.9, 105.8, 60.3, 56.8, 56.3, 36.0. HRMS-ESI calcd for $C_{20}H_{19}NO_2F_3Cl$: 362.1368 [M − Cl]$^+$, found 362.1353.

*5.1.1.17. 6,7-Dimethoxy-2-[2-(4-methoxyphenyl)ethyl]isoquinolinium chloride (**7p**).* Yield: 53%; mp: 122–124 °C; Light yellow solid; ^{1}H NMR (DMSO-d$_6$, ppm): δ 9.56 (s, 1H, 8-CH), 8.51 (d, 1H, *J* = 6.4 Hz, Ph), 8.25 (d, 1H, *J* = 6.4 Hz, Ph), 7.80 (s, 1H, Ph), 7.77 (s, 1H, Ph), 7.74 (s, 1H, Ph), 7.18 (m, 2H, Ph), 6.94 (s, 1H, Ph), 4.83 (t, 2H, *J* = 6.4 Hz, CH$_2$), 4.01 (s, 3H, OCH$_3$), 3.94 (s, 3H, OCH$_3$), 3.68 (s, 3H, OCH$_3$), 3.24 (t, 2H, *J* = 6.4 Hz, CH$_2$). HRMS-ESI calcd for $C_{20}H_{22}NO_3Cl$: 324.1560 [M − Cl]$^+$, found 324.1589.

*5.1.1.18. 2-[2-(4-Chlorophenyl)ethyl]-6,7-dimethoxyisoquinolinium chloride (**7q**).* Yield: 42%; mp: 128–130 °C (decomp); Bright yellow solid; ^{1}H NMR (DMSO-d$_6$, ppm): δ 9.59 (s, 1H, 8-CH), 8.52 (d, 1H, *J* = 6.8 Hz, Ph), 8.26 (d, 1H, *J* = 6.8 Hz, Ph), 7.74 (s, 1H, Ph), 7.69 (s, 1H, Ph), 7.34 (d, 2H, *J* = 8.4 Hz, Ph), 7.24 (d, 2H, *J* = 8.4 Hz, Ph), 4.88 (t, 2H, *J* = 7.2 Hz, CH$_2$), 4.05 (s, 3H, OCH$_3$), 3.99 (s, 3H, OCH$_3$), 3.32 (t, 2H, *J* = 7.2 Hz, CH$_2$). ^{13}C NMR (DMSO-d$_6$, ppm): δ 157.5, 152.4, 145.2, 135.5, 135.2, 133.6, 131.6, 130.8 (2), 128.5 (2), 123.6, 123.1, 107.0, 105.8, 60.5, 56.8, 56.3, 35.6. HRMS-ESI calcd for $C_{19}H_{19}NO_2Cl_2$: 328.1104 [M − Cl]$^+$, found 328.1106.

*5.1.1.19. 6-Hydroxy-7-methoxy-2-(2-phenylethyl)isoquinolinium chloride (**7r**).* Yield: 41%; mp: 224–226 °C (decomp); Yellow solid; ^{1}H NMR (DMSO-d$_6$, ppm): δ 11.96 (s, br, 1H, OH), 9.43 (s, 1H, 8-CH), 8.43 (d, 1H, *J* = 6.8 Hz, Ph), 8.17 (d, 1H, *J* = 6.8 Hz, Ph), 7.58 (s, 1H, Ph), 7.47 (s, 1H, Ph), 7.29–7.19(m, 5H, Ph), 4.80 (t, 2H, *J* = 7.6 Hz, CH$_2$), 3.98 (s, 3H, OCH$_3$), 3.25 (t, 2H, *J* = 7.6 Hz, CH$_2$). HRMS-ESI calcd for $C_{18}H_{18}NO_2Cl$: 280.1338 [M − Cl]$^+$, found 280.1336.

*5.1.1.20. 2-[2-(3-Chlorophenyl)ethyl]-6-hydroxy-7-methoxyisoquinolinium chloride (**7s**).* Yield: 45%; mp: 156–158 °C (decomp); Yellow-green solid; ^{1}H NMR (DMSO-d$_6$, ppm): δ 11.95 (s, br, 1H, OH), 9.46 (s, 1H, 8-CH), 8.43 (d, 1H, *J* = 6.8 Hz, Ph), 8.17 (d, 1H, *J* = 6.8 Hz, Ph), 7.70 (s, 1H, Ph), 7.48 (s, 1H, Ph), 7.43 (s, 1H, Ph), 7.38 (s, 1H, Ph), 7.31 (m, 2H, Ph), 4.42 (t, 2H, *J* = 7.2 Hz, CH$_2$), 3.97 (s, 3H, OCH$_3$), 3.09 (t, 2H, *J* = 7.2 Hz, CH$_2$). HRMS-ESI calcd for $C_{18}H_{17}NO_2Cl_2$: 314.0948 [M − Cl]$^+$, found 314.0957.

*5.1.1.21. 6-Hydroxy-7-methoxy-2-[2-(4-methoxyphenyl)ethyl]isoquinolinium chloride (**7t**).* Yield: 48%; mp: 108–110 °C (decomp); Brown solid; ^{1}H NMR (DMSO-d$_6$, ppm): δ 8.80 (s, 1H, 8-CH), 7.91 (d, 1H, *J* = 6.0 Hz, Ph), 7.49 (s, 2H, Ph), 7.19 (s, 1H, Ph), 7.12 (s, 1H, Ph), 7.10 (s, 1H, Ph), 6.84 (s, 1H, Ph), 6.82 (s, 1H, Ph), 6.72 (s, 1H, OH), 4.50 (t, 2H, *J* = 7.2 Hz, CH_2), 3.82 (s, 3H, OCH_3), 3.72 (s, 3H, OCH_3), 3.12 (t, 2H, *J* = 7.2 Hz, CH_2). HRMS-ESI calcd for $C_{19}H_{20}NO_3Cl$: 311.1521 $[M + H - Cl]^+$, found 311.1509.

*5.1.1.22. 2-[2-(4-Fluorophenyl)ethyl]-6-hydroxy-7-methoxyisoquinolinium chloride (**7u**).* Yield: 37%; mp: 179–181 °C (decomp); Brown solid; ^{1}H NMR (DMSO-d$_6$, ppm): δ 9.26 (s, 1H, 8-CH), 8.26 (d, 1H, *J* = 6.4 Hz, Ph), 7.93 (d, 1H, *J* = 6.4 Hz, Ph), 7.50 (s, 1H, Ph), 8.52 (dd, 1H, *J* = 6.8 Hz, 0.8 Hz, Ph), 8.41 (d, 1H, *J* = 6.8 Hz, Ph), 8.19 (d, 1H, *J* = 6.8 Hz, Ph), 7.80 (dd, 1H, *J* = 8.8 Hz, 2.4 Hz, Ph), 7.60 (d, 1H, *J* = 2.4 Hz, Ph), 7.26 (m, 2H, Ph), 7.10 (m, 2H, Ph), 4.88 (t, 2H, *J* = 7.2 Hz, CH_2), 3.35 (t, 2H, *J* = 7.2 Hz, CH_2). HRMS-ESI calcd for $C_{18}H_{17}NO_2FCl$: 299.1322 $[M + H - Cl]^+$, found 299.1300.

*5.1.1.23. 2-[2-(4-Chlorophenyl)ethyl]-6-hydroxy-7-methoxyisoquinolinium chloride (**7v**).* Yield 28%; mp: 235–237 °C (decomp); Brown solid; ^{1}H NMR (DMSO-d$_6$, ppm): δ 8.68 (s, 1H, 8-CH), 7.80 (d, 1H, *J* = 6.4 Hz, Ph), 7.34 (d, 2H, *J* = 8.0 Hz, Ph), 7.23 (s, 1H, Ph), 7.25 (d, 2H, *J* = 8.0 Hz, Ph), 7.06 (s, 1H, Ph), 6.52 (s, 1H, Ph), 4.48 (t, 2H, *J* = 7.2 Hz, CH_2), 3.80 (s, 3H, OCH_3), 3.17 (t, 2H, *J* = 7.2 Hz, CH_2). HRMS-ESI calcd for $C_{18}H_{17}NO_2Cl_2$: 314.0948 $[M - Cl]^+$, found 314.0964.

*5.1.2. General procedure for N-(2-arylethyl) isoquinolines analogs (**9a**–**c**)*

To a suspension of anhydrous $CuSO_4$ (1.8 equiv) and corresponding hydrochlorate (**5**, 1.0 equiv) in anhydrous formic acid (45 mL) was added 40% glyoxal solution (2.0 equiv) at 100 °C. The reaction mixture was stirred at 100 °C for 1 h. Then the mixture was filtered. The filtrate was concentrated *in vacuo*. The residue (**8**) was acidified and purified to give **9**, and the procedures were similar to those of **7** series.

*5.1.2.1. 2-[2-(3-Chlorophenyl)ethyl]-1,6-dihydroxy-7-methoxyisoquinolinium chloride (**9a**).* Yield 23%; Brown oil; ^{1}H NMR (DMSO-d$_6$, ppm): δ 11.72 (s, br, 1H, OH), 9.04 (s, 1H, Ph), 7.85 (s, 1H, Ph), 7.59 (s, 1H, Ph), 7.54 (s, 1H, Ph), 7.36 (s, 1H, Ph), 7.31 (m, 3H, Ph), 7.16 (s, 1H, Ph), 4.79 (t, 2H, *J* = 7.2 Hz, CH_2), 3.96 (s, 3H, OCH_3), 3.25 (t, 2H, *J* = 7.2 Hz, CH_2). ^{13}C NMR (DMSO-d$_6$, ppm): δ 156.3, 153.0, 151.0, 138.7, 136.4, 133.1, 130.3, 129.2, 127.3, 126.9, 123.3, 122.1, 117.0, 107.6, 104.5, 59.6, 55.3, 36.1. HRMS-ESI calcd for $C_{18}H_{17}NO_3Cl_2$: 330.0891 $[M - Cl]^+$, found 330.0897.

*5.1.2.2. 2-[2-(2-Methylphenyl)ethyl]-1,6-dihydroxy-7-methoxyisoquinolinium chloride (**9b**).* Yield 24%; Dark brown oil; ^{1}H NMR (DMSO-d$_6$, ppm): δ 8.78 (s, 1H, Ph), 7.70 (s, 1H, Ph), 7.59 (s, 1H, Ph), 7.53 (s, 1H, Ph), 7.13 (m, 3H, Ph), 7.05 (d, 2H, *J* = 3.6 Hz, Ph), 4.68 (t, 2H, *J* = 7.6 Hz, CH_2), 4.01 (s, 3H, OCH_3), 3.24 (t, 2H, *J* = 7.6 Hz, CH_2), 2.28 (s, 3H, CH_3). HRMS-ESI calcd for $C_{19}H_{20}NO_3Cl$: 310.1096 $[M - Cl]^+$, found 310.1104.

*5.1.2.3. 2-[2-(3-Fluorophenyl)ethyl]-1,6-dihydroxy-7-methoxyisoquinolinium chloride (**9c**).* Yield: 28%; Dark brown oil; ^{1}H NMR (DMSO-d$_6$, ppm): δ 8.52 (s, 1H, Ph), 7.61 (s, 2H, Ph), 7.44 (s, 1H, Ph), 7.28 (dd, 1H, *J* = 14.4 Hz, *J* = 7.2 Hz, Ph), 7.14 (d, 1H, *J* = 10.0 Hz, Ph), 7.03 (m, 4H, Ph), 4.68 (t, 2H, *J* = 7.2 Hz, CH_2), 3.97 (s, 3H, OCH_3), 3.27 (t, 2H, *J* = 7.2 Hz, CH_2). HRMS-ESI calcd for $C_{18}H_{17}NO_3FCl$: 314.0855 $[M - Cl]^+$, found 314.0842.

5.2. CD36 antagonistic activity

5.2.1. CD36 antagonistic activities on the protein level

Each well of microplates (96-well) was coated with 100 μL oxLDL (5 μg/mL) at 4 °C for 8–12 h. After being washed with phosphate-buffered saline (PBS) buffer twice, the oxLDL-coated wells were blocked with PBS buffer containing 1% bovine serum albumin (BSA) for 1–2 h at 4 °C. The wells were then washed with PBST (PBS buffer with 0.1% Tween-20) buffer twice. After being incubated with 100 μL CD36 (30 μg/mL) or vector control protein at 4 °C for 1 h, 1 μL study compounds (10 μg/mL) or hexarelin (10 μM) was added, respectively. Following 2 h incubation, the plate was washed and incubated with the mouse monoclonal antibody against His-tag protein at a final dilution of 1:1250. The wells were washed and incubated with HRP-conjugated goat antimouse IgG (1:5000 dilution, 4 °C, 1 h). Subsequently, after incubation with 100 μL TMB/H_2O_2 (mixed immediately before incubation by 1:1 [v/v]) for 45 min at 37 °C, 100 μL HCl (1 M) was added to stop the reaction. The optical density (OD) value of each well was recorded using spectrophotometry with the microplate reader (Model 680 microplate reader, Bio-Rad) at 450 nm [17].

5.2.2. CD36 antagonistic activity on the cellular level [18]

Sf9 insect cells were grown and maintained in Grace's medium (Gibco/Invitrogen) supplemented with 10% heat-inactivated fetal bovine serum (TNMFH medium, Hyclone) at 27 °C. Sf9 cells were plated at 6.0×10^5 cells/well in 100 μL of TNMFH medium. After 6 h, the cells were infected with 100 μL of recombinant or wild-type baculoviruses at a multiplicity of infection (MOI) in Grace's medium for 1 h and then refed with 200 μL of TNMFH medium. Two days later, the cells were washed once with Grace medium supplemented with 0.5% (w/v) BSA (Sigma) and refed with 100 μL of BSA. The compounds were dissolved in DMSO and individually transferred (1.1 μL) to the wells to give a final concentration of 10 μg/mL. After 1 h of incubation at 27 °C, DiI-AcLDL (2 μg/mL, Biomedical Technologies) in 8 μL of BSA was added. After 5 h, the fluorescence was measured using a fluorescence microplate reader. Autofluorescence and quenching were tested before removing the incubation medium. After removing the medium, the cells were fixed in 100 μL of 4% polyoxymethylene for 15 min and washed three times with 200 μL of PBS. The cellular uptake of DiI-AcLDL was then determined in 100 μL of PBS. The active results were expressed as the inhibitory percentages of the total DiI fluorescence of Sf9[hCD36] cells incubated in the absence of the compounds:

$$\text{Inhibition rate of total uptake} = \left(\text{Sf9[CD36]}_{\text{compound}} - \text{Sf9[CD36]}_{\text{Ox-LDL}}\right) \Big/ \left(\text{Sf9[CD36]} - \text{Sf9[CD36]}_{\text{Ox-LDL}}\right) \times 100\%$$

5.2.3. CD36 antagonistic activity by fluorescence microscopy

Receptor-mediated endocytosis of DiI-AcLDL by Sf9[hCD36] cells untreated or treated with the compounds **7t** or **7e** (10 μg/mL) were detected by fluorescence microscopy. The cells were treated as described for the Sf9[hCD36] HTS assay and then observed using the IN Cell Analyzer 1000 (GE. Healthcare).

Acknowledgment

This work was supported by the Research Funds of Peking Union Medical College for Young Scientists and the National S&T Major Special Project on Major New Drug Innovation (2009ZX09301-003)

and the National Natural Science Foundation of China (90913002 and 90813027).

References

[1] A.C. Nicholson, S. Frieda, A. Pearce, R.L. Silverstein, Arterioscler. Thromb. Vasc. Biol. 15 (1995) 269–275.
[2] D. Calvo, D. Gómez-Coronado, Y. Suárez, M.A. Lasunción, M.A. Vega, J. Lipid Res. 39 (1998) 777–788.
[3] E.A. Podrez, E. Poliakov, Z. Shen, R. Zhang, Y. Deng, M. Sun, P.J. Finton, L. Shan, B. Gugiu, P.L. Fox, H.F. Hoff, R.G. Salomon, S.L. Hazen, J. Biol. Chem. 277 (2002) 38503–38516.
[4] K.J. Moore, V.V. Kunjathoor, S.L. Koehn, J.J. Manning, A.A. Tseng, J.M. Silver, M. McKee, M.W. Freeman, J. Clin. Invest. 115 (2005) 2192–2201.
[5] J. Han, X. Zhou, T. Yokoyama, D.P. Hajjar, A.M. Gotto, A.C. Nicholson, Circulation 109 (2004) 790–796.
[6] (a) B. Fuhrman, L. Koren, N. Volkova, S. Keidar, T. Hayek, M. Aviram, Atherosclerosis 164 (2002) 179–185;
(b) L. Puccetti, T. Sawamura, A.L. Pasqui, M. Pastorelli, A. Auteri, F. Bruni, Eur. J. Clin. Invest. 35 (2005) 47–51.
[7] F. Bruni, A.L. Pasqui, M. Pastorelli, G. Bova, M. Cercignani, A. Palazzuoli, T. Sawamura, W.R. Gioffre, A. Auteri, L. Puccetti, Clin. Appl. Thromb. Hemost. 11 (2005) 417–428.
[8] N. Ruiz-Velasco, A. Dominguez, M.A. Vega, Biochem. Pharmacol. 67 (2004) 303–313.
[9] C.A. Martin, E. Longman, C. Wooding, S.J. Hoosdally, S. Ali, T.J. Aitman, D.A. Gutmann, P.S. Freemont, B. Byrne, K.J. Linton, Protein Sci. 16 (2007) 2531–2541.
[10] B. Sun, B.B. Boyanovsky, M.A. Connelly, P. Shridas, D.R. van der Westhuyzen, N.R. Webb, J. Lipid Res. 48 (2007) 2560–2570.
[11] M. Febbraio, E.A. Podrez, J.D. Smith, D.P. Hajjar, S.L. Hazen, H.F. Hoff, K. Sharma, R.L. Silverstein, J. Clin. Invest. 105 (2000) 1049–1056.
[12] M. Febbraio, E. Guy, R.L. Silverstein, Arterioscler. Thromb. Vasc. Biol. 24 (2004) 2333–2338.
[13] M. Febbraio, R.L. Silverstein, Int. J. Biochem. Cell Biol. 39 (2007) 2012–2030.
[14] P. Yang, D.-Q. Song, Y.-H. Li, W.-J. Kong, Y.-X. Wang, L.-M. Gao, S.-Y. Liu, R.-Q. Cao, J.-D. Jiang, Bioorg. Med. Chem. Lett. 18 (2008) 4675–4677.
[15] Y.-H. Li, P. Yang, W.-J. Kong, Y.-X. Wang, C.-Q. Hu, Z.-Y. Zuo, Y.-M. Wang, H. Gao, L.-M. Gao, Y.-C. Feng, N.-N. Du, Y. Liu, D.-Q. Song, J.-D. Jiang, J. Med. Chem. 52 (2009) 492–501.
[16] Y.-X. Wang, Y.-P. Wang, H. Zhang, W.-J. Kong, Y.-H. Li, F. Liu, R.-M. Gao, T. Liu, J.-D. Jiang, D.-Q. Song, Bioorg. Med. Chem. Lett. 19 (2009) 6004–6008.
[17] L. Wang, Y. Bao, Y. Yang, Y. Wu, X. Chen, S. Si, B. Hong, J. Biomol. Screen. 15 (2010) 239–250.
[18] Y.-N. Xu, J. Wang, Y. Bao, W. Jiang, L. Zuo, D.-Q. Song, B. Hong, S.-Y. Si, Anal. Biochem. 400 (2010) 207–212.